

A Technical Comparison between Gamma Ray and X-ray CT for Industrial Materials Examination

Susan Sipaun, Hearie B. Hassan, Mohamad Rabaie B. Shari, Airwan Affandi B. Mahmood and Nurliyana Bt. Abdullah

Agensi Nuklear Malaysia, Bahagian Teknologi Industri, 43000 Kajang Bangi Selangor

(Received: 6.8.2021 ; Published: 20.2.2022)

Abstract. Computed tomography (CT) provides a means to non-destructively examine the internals of an object. This work presents two industrial CT systems developed at Agensi Nuklear Malaysia. The x-ray CT and gamma ray CT systems utilise fan-beam and parallel beam configuration respectively and were used in image reconstruction of industrial materials. The x-ray CT consists of GOS linear array detector, rotating table and 160kV X-ray system. Hundreds of projection data were collected on continuous rotation scanning. The gamma CT scanner consists of a mechanical gantry, a 1" x 1" NaI(Tl) scintillation detector, 0.41GBq Ba-133 and 1.67GBq Cs-137 source, 15mm x 5mm lead collimators and Ludlum scaler ratemeter. The selected test materials are commonly found in many industrial plants; insulated pipe, concrete, stainless steel tank and PMMA. The features of the respective CT systems influenced the image output, whereby the x-ray CT system produced images with better resolution, contrast and speed compared to the gamma CT system. However, the gamma CT could provide on-site scanning and is able to image larger and higher density materials.

Keywords: Gamma ray, X-ray, Tomography, Filtered Back Projection

INTRODUCTION

Gamma ray and x-ray computed tomography (CT) systems produce cross-sectional images of objects, which enable users to observe and analyse the objects' internals. Gamma ray CT has been mostly tested in laboratory setups to investigate flow parameters, gas-liquid distribution in pumps, bubble columns and fluidised bed reactor as well as to inspect mock-up pipelines and building pillars for defects [1-8]. Typical radioisotopes used in gamma CT are Am-241 (59.54keV), Ba-133 (356keV), Cs-137 (662keV) with activities ranging from several MBq to a few GBq.

X-ray CT is typically used to make quantitative dimensional analysis in manufacturing and product quality inspection. Industrial x-ray CT systems typically uses x-ray energies between 160kV and 450kV that allows penetration through denser materials like metal and concrete. One of the strategies to scan large objects involved performing scan of the object with the rotary turntable movable along the x-y axis to cover the areas of the object, and combining data images into one [9]. Another strategy utilised slim x-ray tubes that could be placed in tight spaces to inspect aircraft components such as a fibre composite shell of an aircraft [10,11]. Commercial large CT scanner offers options to scan larger and denser components with the use of 9MeV linear accelerator [12,13]. X-ray microtomography, which has a resolution in micrometer range,

is utilised to study microstructure evolution under varying conditions [14]. X-ray has been used together with neutron to image cultural heritage objects [15]. Unlike medical CT usage where patient's exposure is limited to minimise radiation risk, objects of investigation in industrial CT can tolerate higher radiation exposure [16]. Industrial products and materials have a wide-ranging density and higher energy rays are needed to penetrate denser materials compared to the human body. Thus, the industrial CT systems are designed to have the energy range and resolution needed to investigate such materials.

This is paper discusses two CT systems that were developed in Agensi Nuklear Malaysia; 160kV industrial x-ray CT and portable gamma CT systems. The different features of these systems influences the production of CT images for pipe, concrete, metal and plastic.

CT IMAGING

CT images are reconstructed using data from multiple projections [17]. In figure 1, the ionising radiation with intensity, I_0 penetrates the object and loses some energy. Its transmitted rays, I emerge on the other side which is then measured by the detectors. The description of this beam is given in equation (1), where I_0 and I are the intensity of the incident beam and transmitted beam respectively, linear attenuation coefficient, μ and object thickness, x . The ratio corresponds to the attenuation coefficient multiplied by the corresponding path length of all the object elements where the ray traverses. The linear attenuation coefficient, μ is dependent on the given energy, material density and atomic number [18].

$$\ln\left(\frac{I_0}{I}\right) = \mu \cdot x \tag{1}$$

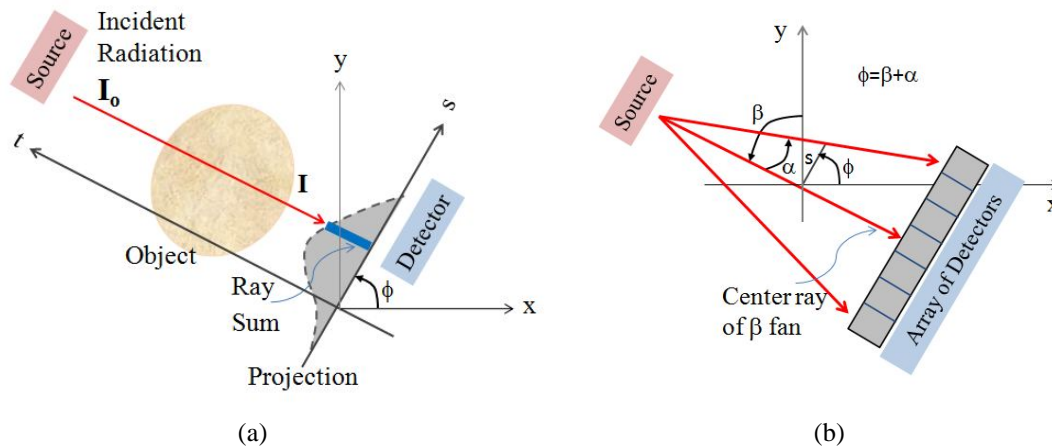


FIGURE 1. CT Data acquisition (a) Parallel beam (b) Fan beam

A CT image is derived from a distribution map of linear attenuation coefficient. In the first generation CT configuration, its data acquisition follows that the single radiation source-detector pair move synchronously at a regular interval along a plane and collects 360° projection data (Figure 1a). Projection function, $P(t_i, \phi_j)$ is defined as a collection of line integrals, t_i through the object along the length, S and at an angle, ϕ_j where i and j are indices for each line integral and

rotation angle respectively. When taken for all ϕ and t , $P(t, \phi_j)$ gives the Radon transform. CT image reconstruction is derived by resolving the image function from a set of projection measurements $P(t, \phi)$ in equation 2, where $x \cos \phi + y \sin \phi = s$ and $I(x, y)$ is the image function.

$$P(t, \phi) = \int_{-\infty}^{\infty} \int_{-\infty}^{\infty} I(x, y) \delta(x \cos \phi + y \sin \phi - s) dx dy \quad (2)$$

The third generation CT configuration in figure 1(b) consists of approximately 1500 detectors and a single x-ray source. The fan-shaped x-ray beam is emitted through the beam collimator. This diverging beam penetrates the object at a selected scanning plane around a 360° rotation. Ray measurements are taken by an array of detectors. This configuration allows faster data acquisition through the usage of equally spaced collinear detectors. Thus, the process of image reconstruction of one section involves implementing the convolution back projection algorithm to produce high quality images. This method is aided by the use of the Fourier Slice Theorem where the one dimensional Fourier transform of the Radon transform along a radial line is identical to the same line in the two dimensional Fourier transform of the object. Image can then be reconstructed from the inverse 2D Fourier Transform. In both parallel and fan beam configurations, the number of projections influences the degree to which we can discern the fine details of the image structure. In general, the higher the number of projections, the better the image resolution.

Gamma Ray CT

The gamma CT scanner consists of a motorised mechanical gantry, a 1" x 1" NaI (Tl) scintillation detector, gamma source, 15mm x 5mm lead collimators and Ludlum scaler ratemeter. The scintillation detector was chosen due to its stopping efficiency. Collimation defines the volume in the object to be illuminated by the source and it is this volume viewed by the detectors. A suitable gamma ray source was used to scan the industrial samples. Barium-133 with activity 0.079GBq was used to scan the insulated 2" pipe, 6cm diameter cylindrical concrete and 20cm diameter PMMA phantom that comes with 25, 19, 12, 10, 8, 3mm holes. For the stainless steel tank 70cm diameter and cylindrical cement 10cm diameter with 16mm metal rod, the 1.67GBq Cs-137 was used. The sample was placed within the scanner's field of view. Data was collected via translate-rotate configuration and the source and detector moved synchronously. Data is collected at every 2.5mm translate interval, and rotation at 5° for angles 0° to 180°. For the 70cm tank, 1cm translate interval was used. Translation scanning length was set at 16cm (pipe), 20cm (concrete cylinder) and 80cm (tank) respectively. Scan time is defined as the time taken to complete data acquisition. CT data is first collated and rearranged using a dedicated program, Konversi03, to build sinograms. CT image is then reconstructed using filtered back projection algorithm in another dedicated program, Reconstructor03 [19, 20].

Industrial X-ray CT

The main components of the industrial CT system consist of a 160kV/10mA x-ray machine with 0.4 focal spot (IEC336), rotary table and linear array detector (Figure 3). The emergent fan

beam angle is 40° with 5mm beam size output at source. Source to detector distance is approximately 1 meter. The x-ray output with current stability 0.05%/h was stable throughout the time taken for sample scans, which is the time taken by the mechanical movements and data acquisition. Scanning was carried out for insulated pipe and cylindrical cement mix at 130kV/5mA and 160kV/10mA respectively.

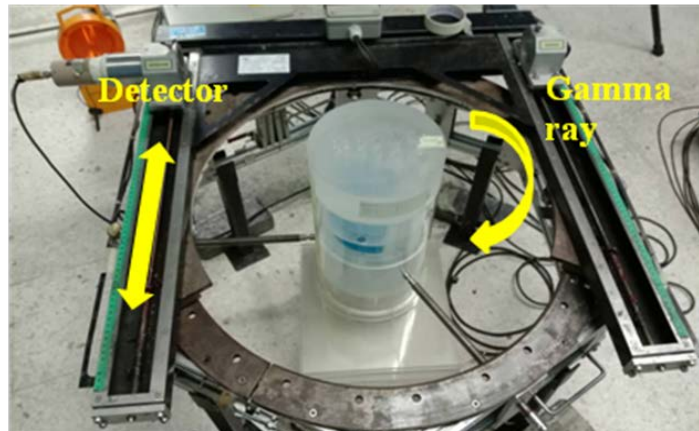


FIGURE 2. Gamma ray CT system: parallel beam, translate-rotate

The linear array detector (LAD) has gadolinium oxysulfide (GOS) as the scintillator material mounted on the surface of an array of photodiode. X-rays incident upon a scintillator are converted to visible light, which is then picked up by the detector front-end (pre-amplifier and multiplexer) and A/D conversion of the signal is through its amplifier stages. The control unit houses the control and digital signal processing electronics whereas a frame grabber is used to transform detector data into images. The LAD is enclosed in a metal casing that is installed with x-ray beam collimator and x-ray shielding for the electronics. The LAD has a high dynamic range using a 14bit ADC resolution. The pixel size is 0.6mm (H) x 0.3mm (W) and 0.4mm pitch. The active length is 614mm and the optimum length is selected so that it covers the circle of reconstruction. The user performs calibration of the detector elements and subsequently initiates the LAD. The sample is placed on the rotary table for scanning. Image grabbing is triggered by a signal by the user and data is acquired every 0.5° to obtain 720 projections [21-24].

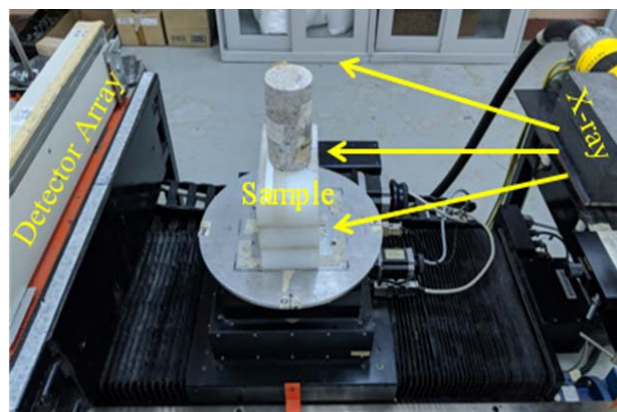


FIGURE 3. X-ray CT system: fan-beam, rotate only

RESULTS AND DISCUSSION

CT scans were performed using both gamma and x-ray CT systems. The steps involved in one complete scan are sample preparation, scanner setup and parameter selection, data acquisition and processing, and finally image reconstruction and analysis are performed. Differences in material density within the investigated objects provided image contrast in dark, white and grey shades. Dark shades indicate the material of relatively lower density, such as air gaps or voids, compared to metal pipe density; white indicates the material of higher density (metal rod); grey shades indicate moderately dense material.

Scan Observations

For the purpose of comparison between the two CT systems, scan data of two samples, insulated pipe and cement mixture, were obtained and visualised. Figure 4 shows a picture of the insulated pipe, concrete and their respective CT images. Reasonable image quality was achieved in terms of the ability to discriminate shape, structure and density. It is clear to see that the x-ray CT system that obtained 720 projections performed much better compared to gamma ray CT which only had 37 projections. One of the design dilemmas of this prototype gamma CT system is achieving the balance between system size, resolution, portability and cost. The use of sodium iodide detector in the gamma CT system is well justified due to its detection efficiency and resolution for energy range between 511 and 1132keV. It can also tolerate temperatures between 25 and 100 Celsius and still perform detection reliably in the lab or at an outdoor inspection site. The size of the current NaI(Tl) detector is 1" x 1" (25.4mm length x 25.4mm diameter). An array of this type of detector will use a relatively large space in an imaging system, and increases the cost of building the CT system. Therefore a single detector was chosen instead, however, this selection limits the number of projections that could be obtained within the fixed gantry. To increase the number of projections one may use many smaller detectors to maximize the number of detectors in the imaging system. The cross-sectional pipe image is most clear with the x-ray CT, where the outer aluminium sheet cover is seen as a light grey, mild steel pipe is almost white and the metal rivet white. The calcium silicate insulation (2.9 gcm^{-3}) and air (0.0012 gcm^{-3}) are both in shades of dark grey. The shapes are clear, however, we can see dark streaks at the rivet due to beam hardening and scatter. The gamma CT image for the same pipe sample came with artifacts where only air and mild steel pipe can be distinguished. The CT image does not show the rivet, insulation and aluminium but instead a mixture of streaks and white spots appear. It is due to Ba-133 being relatively high energy for small-sized lower density materials. Therefore a dual energy system using both Ba-133(356keV) and Am-241 (59keV) may be more suitable to resolve mix density materials. In the CT analysis of a 10mm diameter concrete sample, Am-241 3.7GBq (100mCi) was used to scan through stone and voids, and could reliably resolve its composition [26]. For the cylindrical concrete mix, both x-ray and gamma ray cross-sectional images can reproduce the circular shape as well as discriminate the aggregates within the cement. X-ray CT provided better contrast and resolution due to it having smaller and more detectors compared to the single gamma detector.

One of the limitations of the single detector setup is having long scanning times. The scanning time is defined as the total time taken by the mechanical movements as well as electronic data acquisition. In terms of scan time, the x-ray CT took several minutes compared to several hours

with gamma CT. This is due to the x-ray system acquired data on rotation only and had an array of detectors compared to gamma ray CT system that had single source-single detector configuration on translate-rotate scan motion. The advantages of gamma CT over x-ray CT are portability, lower cost and ability to use a wide range of radioisotope energies without many changes to the system setup. While the x-ray CT is a fixed system, the gamma CT is portable and can be brought to any site, is battery-operated or alternatively can be operated using a generator.

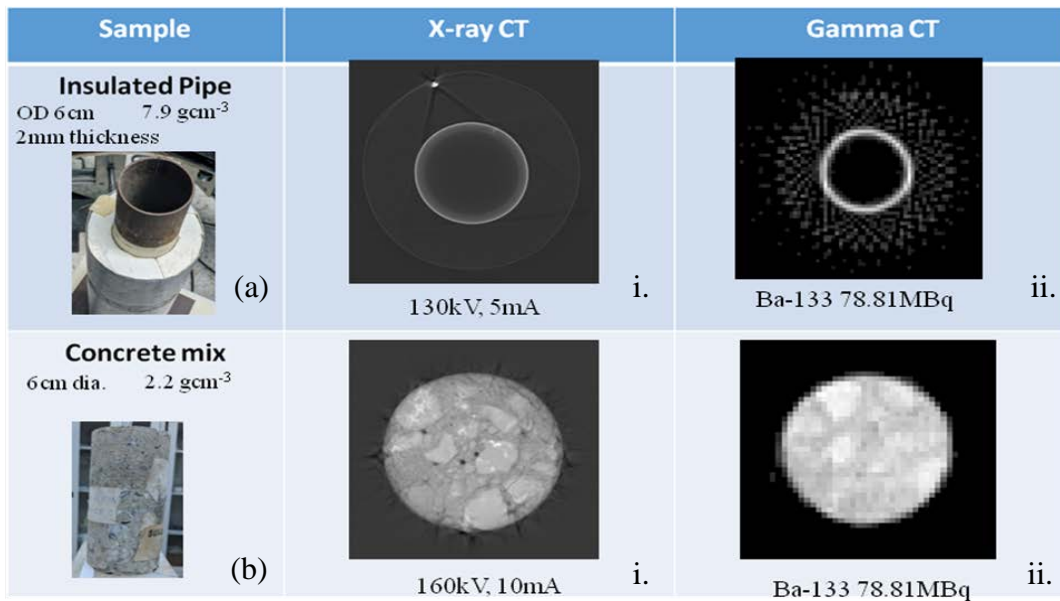


FIGURE 4. (a). An empty insulated pipe sample consists of mild steel, calcium silicate and aluminium jacket. Figures 4(a)i and 4(a)ii show the pipe's x-ray and gamma ray cross sectional images respectively. (b). A core sample of building concrete consists of cement and aggregates. Figures 4(b)i and 4(b)ii show the core's x-ray and gamma ray cross sectional images.

Image Fidelity to Object

Figure 5 shows three objects with their respective cross sectional images. These CT images were obtained using the portable gamma CT system. The phantom is made of PMMA material or 'Perspex' and has twelve holes. Its image shows clearly ten holes and another two smaller holes are not seen. This is due to the scanning plane being at a height where it does not pass through them. The holes with 25, 19, 12, 10, 8mm diameters were made to be at the same depth, but the 3mm holes were shorter and therefore do not show up in the image. The image reconstruction for the cylindrical concrete with metal rod was reasonably resolved with minimal blurring. This blurring shows up at the cement-air and cement-metal interfaces. The white dot represents metal and the grey shade is the concrete mix, although the aggregates within the mix are not visible due to being less sensitive to similar densities; gravel and cement densities are approximately 1.68 gcm⁻³ and 1.4 gcm⁻³ respectively. The stainless steel (SS) tank with seven SS heater rods is a mock-up nuclear fuel assembly [25]. The scan plane was at a height where only the tank and the seven rods are selected for imaging. Its image reveals all seven rods and the tank shape is clearly distinguished. Artifacts appearing as white streaks are mainly due to differences in material

density, SS (7.9 gcm^{-3}) and air (0.0012 gcm^{-3}). Using two energies, for example Cs-137 (662keV) and Am-241 (59keV), in the same CT system could improve the image quality by having the lower energy rays more sensitive to lighter materials. Adding more projections to gamma CT is expected to improve resolution and minimise blurring.

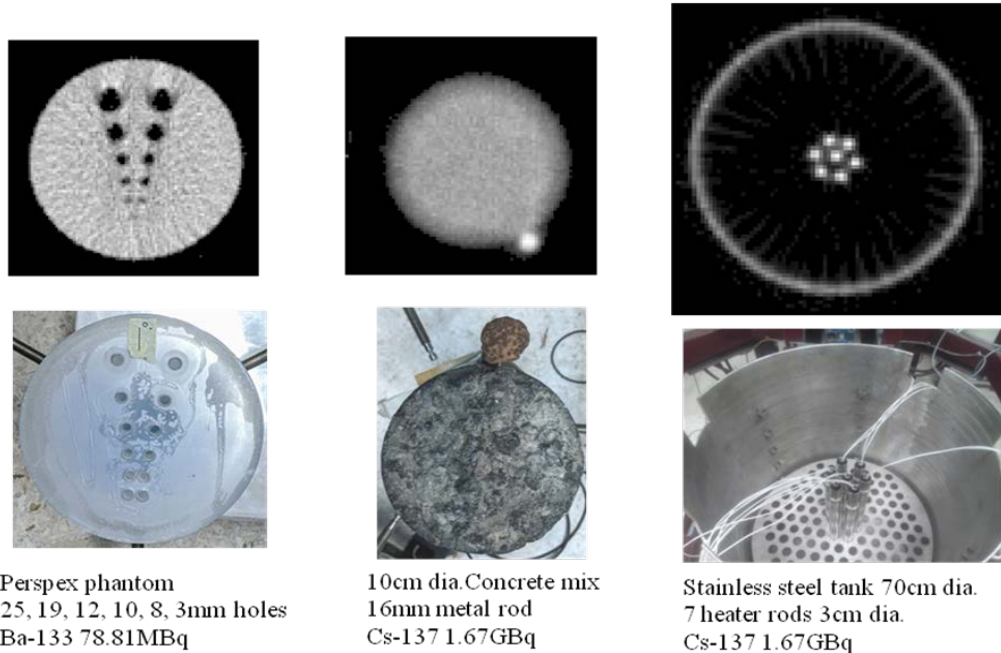


FIGURE 5. Gamma ray CT images

CONCLUSION

CT scans were carried out using dedicated x-ray CT and gamma ray CT scanners to produce cross sectional images of several industrial materials. An insulated pipe and a cement mix were chosen for scanning and imaging to test out the CT systems' technical specifications. Due to the x-ray system having a more superior setup compared to the gamma CT, it was found that reconstructed images produced by it were well resolved, has better contrast and faster scanning time. However, the gamma CT could provide on-site scanning and is able to image larger and higher density materials at reasonable resolution and contrast. Both systems showed that they can produce realistic image fidelity to the object's shape and material relative densities. The cross sectional images were able to show contrast between low and high density materials within the objects. These systems are suitable for use in industrial material examination to resolve heterogeneous mixtures.

ACKNOWLEDGMENTS

The authors thank the staff of Bahagian Sokongan Teknikal (BST) for work on the mechanical and data acquisition modules and Bahagian Teknologi Industri for CT system development and sample preparation. This work is a part of the "Development of portable gamma CT system for on-site large object scanning" project, NM-R&D-21-62 (2020-2021). The research leading to these results has gratefully received funding from IAEA through TC Project

MAL8019 "Development of Industrial Process Gamma-ray and X-ray Tomography" and Nuklear Malaysia Trust Fund.

REFERENCES

1. Industrial Process Tomography. IAEA-TECDOC-1589, IAEA Vienna 2008. ISBN 978-920-0-104508-9
2. G.A. Johansen, "Gamma Tomography" in [Industrial Tomography](#) Systems and Applications Woodhead Publishing Series in Electronic and Optical Materials, 2015, Pages 197-222
3. C. H. de Mesquita, D. V. de Sousa Carvalho, R. Kirita, P. A. S. Vasquez, M. M. Hamada. Radiation Physics and Chemistry 95(2014) 396–400
4. A. Efhaima A, M.H. Al Dahhan. Hydrodynamics study in a fluidized bed reactor using gamma ray computed tomography (CT) technique. Int J Petrochem Sci Eng . 2016;1(4):92-96. DOI: [10.15406/ipcse.2016.01.00017](https://doi.org/10.15406/ipcse.2016.01.00017)
5. D.H. Lee, C. Park, C.H. Baek, C. Lee, S.J Lee, H. Song, and Y.H. Chung. IEEE Transactions on Nuclear Science, Vol. 64, No. 10, October 2017
6. D. N. The Duy, N. H. Quang, P. V. Dao, B. T. Duy, N. V. Chuan. 77:17 (2015) 49–53 eISSN 2180–3722
7. S. Xin and H.X. Wang. Review of Scientific Instruments 88, 025106 (2017)
8. S. Sipaun, M. F. Ab Rahman, N. A. Masenwat and H. Hassan. Proceedings of the 14th Asia-Pacific Physics Conference. AIP Conf. Proc. 2319, 080016-1–080016-4; <https://doi.org/10.1063/5.0036993>
9. E.A. Sivers. Nuclear Instruments and Methods in Physics Research B 99 (1995) 761-764
10. U. Ewert, B. Redmer, C. Rädcl, U. Schnars, R. Henrich, K. Bavendiek and M. Jahn, "Mobile Computed Tomography for Inspection of Large Stationary Components in Nuclear and Aerospace Industries" in Materials Transactions, Vol. 53, No. 2, 308 to 310 (2012) <https://doi.org/10.2320/matertrans.I-M2011848>
11. T. Schäfer, A. Bieberle, M. Neumann, U. Hampel. Flow Measurement and Instrumentation, Volume 46, Part B, December 2015, Pages 262-267
12. Cairnhill X-ray CT Inspection and Metrology: Power|Scan HE. website <http://www.cairnhill.com/Products>. Accessed 9 June 2021
13. Baker Hughes Phoenix X-ray: 9MeV High Energy CT Inspection. website <https://www.bakerhughesds.com/waygate-technologies/radiography-ct/high-energy-ct-inspection> Accessed on 9 June 2021
14. H. Basri, A. T. Prakoso, M. A. Sulong, A. P. Md Saad, M. H. Ramlee, D. A. Wahjuningrum, S. Sipaun, A. Ochsner and A. Syahrom. Mechanical degradation model of porous magnesium scaffolds under dynamic immersion. Proceedings of the Institution of Mechanical Engineers Part L Journal of Materials Design and Applications 234(1):146442071988173
15. D. Mannes, F. Schmid, J. Frey, K. Schmidt-Ott, E. Lehmann. Physics Procedia 69 (2015) 653 – 660
16. W. Huda, CT Radiation Exposure: An Overview. Curr Radiol Rep 3, 80 (2015). <https://doi.org/10.1007/s40134-014-0080-x>
17. A.C. Kak and M. Slaney, Principles of CT imaging. IEEE Press ISBN 0-87942-198-3, 1988.
18. J. H. Hubbell and S. M. Seltzer. X-ray Mass Attenuation Coefficients NIST Standard Reference Database 126

19. J. Abdullah, S.M. Sipaun, M. K. M. Said, G. H. P. Mohamad, M. Ibrahim, I. Mustapha, R. M. Zain, M. F. A. Rahman, M. Mustapha, M. R. Shaari and H. Hassan. "Development of an x-ray computed tomography system for non-invasive imaging of industrial materials" in AIP Conference Proceedings 1017, 408 (2008); <https://doi.org/10.1063/1.2940672>
20. M. Ibrahim, J. Abdullah, N. Yussup, N.A. A. Rahman, M. Mokhtar, H. Ithnin and H. Hassan. Development of Software for automation and Data Acquisition System for Gamma Spider and SPECT. <https://inis.iaea.org/collection/NCLCollectionStore/>
21. S.M. Sipaun and J. Abdullah, "Aspects of x-ray tomographic imaging", Young Researchers Conference on Applied Sciences (CAS 2006) Proceedings, UiTM Shah Alam, Malaysia, 2006, pp. 123-127
22. J. Abdullah, H. Hassan, M. R. Shaari, S. Mohd, M. Mustapha, A. A. Mahmood and S. Jamaludin. Optical Engineering 52(3), 036502 (2013)
23. J. Abdullah, H. Hassan, M. R. Shari, M. Mohd Ibrahim, N. Yussup, H. Ithnin, A. A. Mahmood., Jurnal Teknologi, Vol 77, No 17 Special Issue on Sensor Technology and Control System Applications, 3 (2015)
24. Detection Technology, X-ray linear array detector X-Scan f3 series general characteristics, 2008.
25. S. Sipaun, A. A. Mahmood, M. F. A. Abdol Azis, M. R. Shari, H. Hassan, N. Abdullah, "Design Development of Heater Tank Rod Assembly" in Nuklear Malaysia Technical Convention (NTC) Proceedings, 2019.
26. J.M de Oliveira, A.C.G. Martins and J. A. DE Milito. Brazilian Journal of Physics, Vol. 34, No.3A, 1020-1023 (2004).